Metal-insulator transition of the $LaAlO_3$-$SrTiO_3$ interface electron system

Y. C. Liao,[1] T. Kopp,[1] C. Richter,[1] A. Rosch,[2] and J. Mannhart[1,*]

[1]*Experimental Physics VI, Center for Electronic Correlations and Magnetism, Institute of Physics, University of Augsburg, D-86135 Augsburg, Germany*

[2]*Institute of Theoretical Physics, University of Cologne, D-50937 Cologne, Germany*

(Received 2 October 2010; published 2 February 2011)

We report on a metal-insulator transition in the $LaAlO_3$-$SrTiO_3$ interface electron system, of which the carrier density is tuned by an electric gate field. Below a critical carrier density n_c ranging from 0.5 to 1.5 $\times$ $10^{13}/cm^2$, $LaAlO_3$-$SrTiO_3$ interfaces, forming drain-source channels in field-effect devices, are nonohmic. The differential resistance at zero channel bias diverges within a 2% variation of the carrier density. Above n_c, the conductivity of the ohmic channels has a metal-like temperature dependence, while below n_c conductivity sets in only above a threshold electric field. For a given thickness of the $LaAlO_3$ layer, the conductivity follows a $\sigma_0 \propto (n - n_c)/n_c$ characteristic. The metal-insulator transition is found to be distinct from that of the semiconductor 2D systems.

DOI: 10.1103/PhysRevB.83.075402 PACS number(s): 73.23.−b, 73.20.−r, 73.40.−c, 73.43.Nq

I. INTRODUCTION

Conducting electron systems with unique properties can be generated at interfaces between highly insulating oxides, the most widely studied case being the interface between the TiO_2-terminated (001) surface of $SrTiO_3$ and $LaAlO_3$ (Ref. 1). This electron system behaves as a two-dimensional (2D)[2–5] electron liquid[6] for which superconducting[7] and magnetic ground states[8] have been reported. At low temperatures, the interface can be tuned from a superconducting to a resistive state by applying transverse electric fields.[9] At higher temperatures, large electric gate fields drive the system through a metal-insulator transition (MIT).[10,11]

The $LaAlO_3$-$SrTiO_3$ 2D system is disordered.[12,13] The disorder arises, for example, from dislocations crossing the interface or from point defects. Consequently, as a 2D electron system (2DES), the interface is expected to be an insulator for $T = 0$ K, at least for negligible interaction strength among the electrons.[14] The observed metallic behavior may be interaction driven or a crossover effect; sizable interactions have indeed to be anticipated due to the large interaction energy at small carrier densities.[15,16] Indeed, for the 2DES of semiconductor interfaces[17,18] it has been argued[19] that the metallic phase is not a Fermi liquid because a fictitious electron system with suppressed electronic correlations would form a localized phase[14] rather than a 2D Fermi gas. The polar nature of the $LaAlO_3$-$SrTiO_3$ interface possibly results in additional defects and excitations. Excitations of localized electrons and charged defects, for example, can enhance dephasing and thereby reduce weak localization.

The MIT at semiconductor interfaces is still being debated intensely.[20–25] The discovery of an MIT at the interface of perovskite oxides, an entirely different host structure for a 2DES, may shed light on the nature of the MIT in two dimensions. In previous experiments[10,11] the MIT was deduced from the suppression of the conductance, but has not been investigated further.

In field-effect studies of the perovskite interfaces, the gate fields were considered to change the properties of the electron system primarily by altering the carrier density n. It has recently been revealed, that by compressing the electron wave function toward the interface, the field also changes the effective disorder of the system and therefore its electronic mobility μ (Ref. 26).

To advance these issues further, we have measured the current-density vs. electric-field characteristics $[J(E)]$ of the interface electron system as a function of applied gate fields. These studies show that in the samples investigated the effects of the gate fields have a strong component that arises from a change of n. The data furthermore reveal a power-law behavior of the conductivity σ of the 2D electron liquid as function of n.

II. EXPERIMENT

For the measurements we have fabricated seven samples with thicknesses of the $LaAlO_3$ layers of 4 and 8 unit cells (uc) to investigate a possible dependence of the field effects on the $LaAlO_3$ thickness. The thickness of 4 uc was chosen to yield the critical thickness required for interface conduction.[10] The samples were fabricated by epitaxially growing $LaAlO_3$ layers on the (001) surfaces of TiO_2-terminated,[27,28] 1-mm-thick $SrTiO_3$ single crystals. Scanning force microscopy was used to verify that the substrate surfaces were atomically flat. The films with a nominal composition of $LaAlO_3$ were grown by pulsed laser deposition from a single crystalline $LaAlO_3$ target using standard deposition conditions (780°C, 7 $\times$ 10^{-5} mbar O_2). By reflective high-energy electron diffraction the thickness of the $LaAlO_3$ layers was controlled with a precision of ∼0.1–0.2 uc. After growth, the films were annealed for an hour in 400 mbar O_2 to minimize oxygen vacancies. The devices were photolithographically patterned[29] into the structure shown in Fig. 1. This structure was optimized for Hall measurements and for four-point measurements of the $J(E)$ characteristics, using a small distance between the voltage contacts to minimize the inhomogeneity of the gate fields. Contact pads for the voltage and current leads were prepared by sputtering Ti into holes Ar-ion etched through the $LaAlO_3$. The back gate was provided by silver diffused into the $SrTiO_3$.

Due to the patterning process used,[29] the conducting channels of the interface are separated from each other by

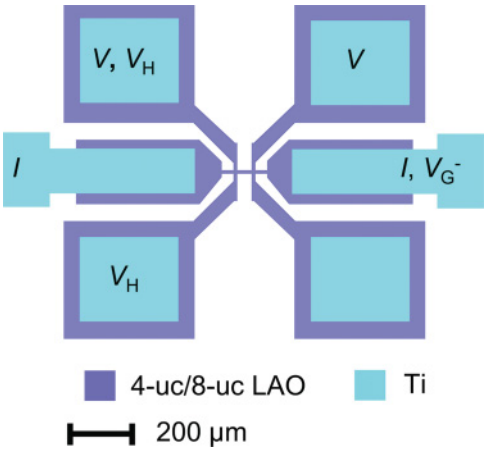

FIG. 1. (Color online) Sketch of the sample structure (top view).

insulating areas (sheet resistance >10 GΩ). These only differ from the conducting areas by the thickness of the $LaAlO_3$ layer (two unit cells instead of, e.g., four), making us conclude that the conductivity of the channel is not induced by a standard doping process, such as doping by oxygen vacancies or by interdiffusion.

For each gate voltage (V_G) the $J(E)$ characteristic in zero magnetic field, Hall voltages and the magnetoconductances at several gate voltages were measured. The Hall voltages varied linearly with the applied magnetic field, except for samples with high carrier densities ($n > 3 \times 10^{13}/\mathrm{cm}^2$) at low temperatures ($T < \sim 50$ K) and large fields ($H > \sim 5$ T). Gate leakage was always below 1 nA. Only negative gate voltages were applied, for these characteristics were found to be reversible with n.

III. RESULTS AND DISCUSSION

The $J(E)$ characteristics are displayed in Fig. 2. Due to the four-point geometry used, the $J(E)$ characteristics are expected to characterize the transport properties of the interface rather than to be influenced by space-charge effects possibly occurring at the contacts. At small J and small $|V_G|$ ($V_G \geqslant -61.2$ V, 4 K) the characteristics are linear for the whole range of J and for $T < 50$ K. At larger $|V_G|$ ($V_G < -61.2$ V, 4 K), however, the $J(E)$ characteristics are nonlinear, showing an enhanced differential resistance for small currents [Fig. 2(a)]. For $V_G < -62.1$ V [Fig. 2(b)], the curves are characterized by a clear threshold behavior: below a characteristic threshold field E_{th}, the current density is extremely small (<2 μA/cm) and displays a weak hysteretic behavior, which is caused by the RC time constant of the measurement. The size of the hysteresis loop shrinks to zero when the measuring time is long enough. Because these current densities are minute, we cannot rule out that they are affected by finite gate currents. Figure 2 therefore shows that the interfaces are insulating at the low carrier densities corresponding to $V_G < -62.1$ V. Significant conductivity is found only above E_{th}. Above E_{th} the current grows nonlinearly. The width E_{th} diminishes with increasing n to approach zero at a critical density $\sim n_c$ (Fig. 3) defined below.

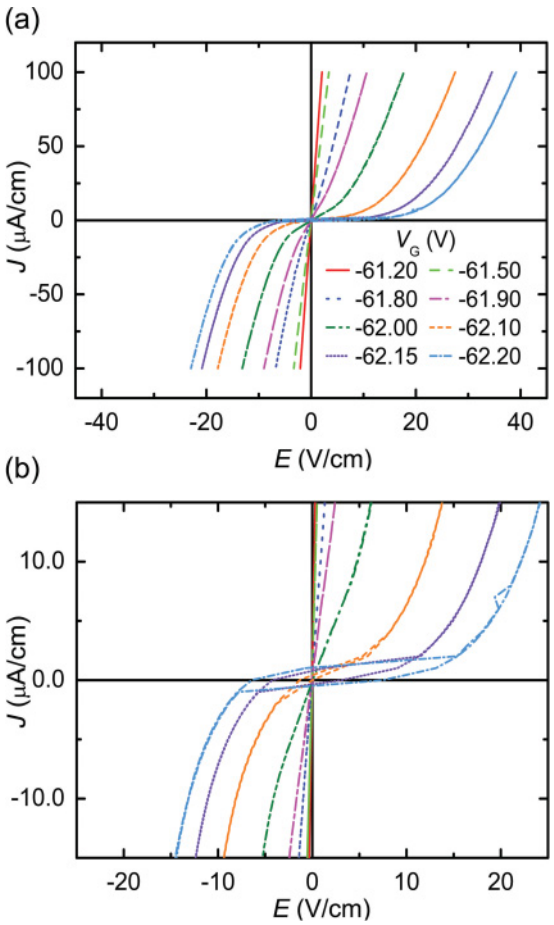

FIG. 2. (Color online) (a) $J(E)$ characteristics of a measurement bridge in a $LaAlO_3$-$SrTiO_3$ interface with a 4-uc-thick $LaAlO_3$ layer (4 K, no applied magnetic field). The bridge was 60 μm long and 10 μm wide. At $V_G = -61.2$ V, the $J(E)$ characteristic changes from linear to nonlinear behavior with a much smaller conductivity. At $V_G = -62.1$ V, the differential conductivity at $J \sim 0$ equals $\sim 10^{-7}$ S. (b) $J(E)$ characteristics of (a) plotted in the small current regime. For $V_G \leqslant -62.1$ V a hysteresis emerges near zero bias and conductivity sets in only above a threshold field E_{th}. This hysteresis is caused by the long RC time in this regime and shrinks to zero on increasing the time constant of the measurement. Because in the insulating regime the voltage V along the bridge is no longer small compared to V_G, the respective $J(E)$ characteristics are asymmetric. The color code is the one of (a).

The conductivity curves bear the characteristic shape shown in Fig. 4(a) for the 4-uc-thick samples in zero magnetic field. The 8-uc-thick samples display a similar, but noisier, behavior (shown in the appendix). For $n \geqslant 2 \times 10^{13}/\mathrm{cm}^2$ the conductivity at zero bias σ_0 decreases approximately linearly with n. As long as the samples show linear[30] $J(E)$ characteristics, e.g., at $V_G > -61.2$ V (Fig. 2), their conductivities are at least of order e^2/h. Conductivity values with $\sigma_0 \lesssim e^2/h$ that are plotted in Fig. 4(a) were obtained from nonlinear characteristics and present the differential conductivity at zero bias (σ_0). For $n < n_c \sim 0.5$–$1.5 \times 10^{13}/\mathrm{cm}^2$ (depending on sample and temperature), however, σ_0 collapses and the samples are effectively insulating (Fig. 2), unless an in-plane electric field $E > E_{\mathrm{th}}$ is applied. The transition from

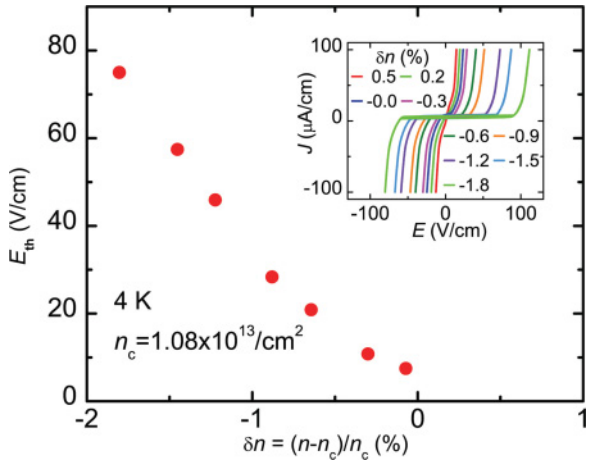

FIG. 3. (Color online) Threshold electric field $E_{\rm th}$ as shown by Fig. 2 plotted as function of the reduced carrier density $\delta n = (n - n_c)/n_c$. The inset shows the respective $J(E)$ curves.

the insulating to the linear regime occurs within ∼0.02 n_c and is reversible with n. The Hall mobility $\mu \equiv \sigma/ne$ is small near the transition, equaling ∼30 cm^2/Vs and ∼5 cm^2/Vs as calculated in the linear regime for the 4- and 8-uc-thick samples, while outside the transition μ reaches 1000 cm^2/Vs.

Overall, the temperature dependence of the conductivity is surprisingly weak and can, to a large extent, be absorbed into a simple shift of the curves along the n axis. For all samples of a given thickness we therefore find that the $\sigma(n)$ characteristics in the ohmic regime can be scaled onto a master curve [Fig. 4(b)]. In this figure the conductivity σ_0 is plotted as a function of the reduced carrier density $\delta n = (n - n_c)/n_c$. The values of n_c depend on temperature and are given in the appendix. For $0.05 < \delta n < 1$, in this range $\sigma_0 > e^2/h$, the master curve is characterized by a power-law behavior $\sigma_0 \propto \delta n^q$, with $q \sim 1$. Interestingly, the interfaces follow this characteristic curve for the whole temperature range for which the experiments could be performed (3 K $< T <$ 50 K), although the dielectric constant of $SrTiO_3$ is temperature dependent. While the data of the 8-uc samples are characterized by considerably larger scatter, for $0.05 < \delta n < 1$ they approach the curve of the 4-uc-thick samples (shown in the Appendix).

In the vicinity of the MIT, within a 2% variation of the carrier density, the data scatter more and the zero-bias differential conductivity deviates from a power-law dependence, when $\sigma_0 < e^2/h$. Similarly, on the insulating side a decrease of n by just 1 or 2% causes substantial threshold fields (Fig. 3).

For an analysis of the behavior close to the MIT, it is suggestive to compare the 2DES of $LaAlO_3$-$SrTiO_3$ interfaces to the 2DES of semiconductor interfaces,[17,18,20,24] for which many different scenarios have been discussed; see, e.g., Refs. 19–24. In these semiconductor systems, the transition is controlled by *two* parameters, temperature and density, whose interplay can be described by a single-parameter scaling function, $\sigma(\delta n, T) = f(\delta n/T^{1/\nu z})$, where ν is the correlation length exponent, and z the dynamical critical exponent. These exponents are usually of the order of 1. In contrast, the conductivity of the $LaAlO_3$-$SrTiO_3$ interfaces is primarily controlled by δn; the temperature has very little influence and accordingly such a scaling relation is not found. In this respect, the MIT is not comparable to that of the semiconductor interfaces. Moreover, the $J(E)$ characteristics for $n < n_c$ display a threshold behavior with a subsequent $J(E) \propto (E - E_{\rm th})^2$ dependence which has not been observed for the semiconductor interfaces.

Several candidates of possible insulating states exist. The first candidate is an Anderson insulator, in which single electrons are localized by disorder. The second candidate arises, if Coulomb interactions are strong; the electrons then form a Wigner crystal which is pinned by disorder. The third candidate is a polaronic insulator; strong electron-phonon interaction can lead to a self-trapping and localization. One of our surprising results is the absence of significant temperature dependencies of the $J(E)$ characteristics in combination with strong nonlinear effects from moderate electric fields. In a typical electric field of 10 V/cm, an electron has, for example,

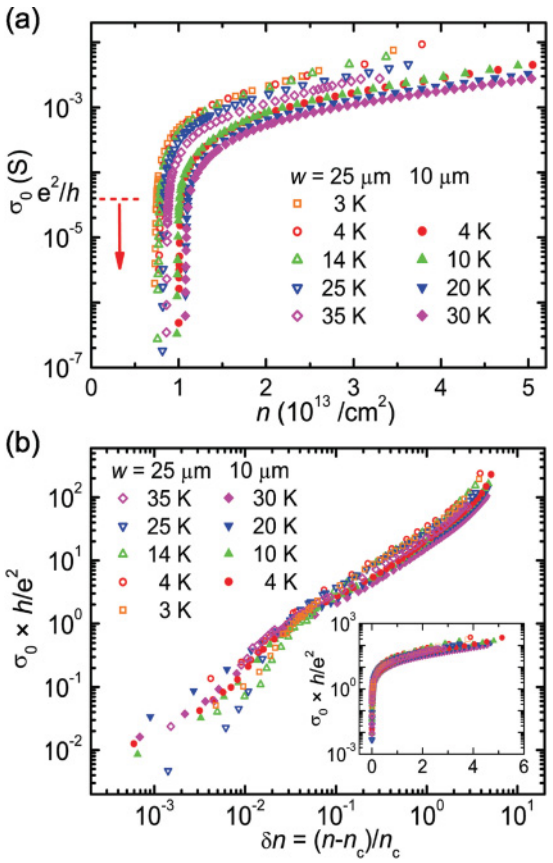

FIG. 4. (Color online) (a) Conductivities of 10- and 25-μm-wide channels in 4-uc $LaAlO_3$-$SrTiO_3$ interfaces measured as function of the carrier density varied by V_G (in zero magnetic field). For $\sigma_0 \lesssim e^2/h$, the current-voltage characteristics are nonlinear. Only data points derived from $J(E)$ curves that are reversible for the whole bias range are plotted. (b) Conductivities of $LaAlO_3$-$SrTiO_3$ interfaces plotted as function of the reduced carrier density. The scaling curve only includes data points in the ohmic regime. For $\delta n = 0$, σ_0 becomes minute (inset).

to travel about 1 μm, more than 100 times the typical distance of electrons at n_c, to gain an energy of k_BT (for $T = 10$ K). The effective absence of thermal effects therefore implies that either barriers prohibiting transport are macroscopic in size or that the motion of electrons is controlled by a collective effect in which many electrons participate as is, e.g., the case in a Wigner crystal. Indeed, the characteristic dependence of the conductivity on the electric field is known from the depinning of two-dimensional vortex lattices in superconducting films.[31] Also simple estimates[16] suggest that Coulomb interactions can be sufficiently strong to induce Wigner crystallization, especially if one takes into account that polaronic effects may enhance the tendency to crystallization.

A possible scenario is therefore that at the MIT an insulating phase, such as a pinned Wigner crystal, percolates through the system. Remarkably, the MIT has been related to a percolation transition also in semiconductor systems.[21,25] The critical conductance exponent of a percolation transition in 2D is 1.3, in conformity with our findings. For the low electronic densities in the semiconductor systems, the transition is possibly induced through scattering by unscreened impurity charges.[25] For the $LaAlO_3$-$SrTiO_3$ 2D system the charge density of order $10^{13}/cm^2$ is so high that it may preclude the observation of a percolation transition driven by unscreened impurity charges. An alternative possibility is a transition where a Wigner crystal or another phase, e.g., a glassy state induced by strong Coulomb interactions,[22] melts. It is also noted that for oxide materials n_c is a small carrier density. The carrier injection induced by an electric field $E > E_{th}$ causes a nonequilibrium state with a carrier density that is locally enhanced. We therefore regard it as a possibility that the MIT is influenced or even triggered by macroscopic inhomogeneities in the sample, as, for example, induced by the enhanced carrier density at the contacts. This could also affects the $J(E)$ dependencies, causing nonlinearities.

To illustrate the characteristics of the $LaAlO_3$-$SrTiO_3$ interface above the MIT, typical magnetoconductance curves are shown in Fig. 5. At high carrier density, the $\Delta\sigma/\sigma$ characteristics exhibit a $-H^2$ dependence (red curve), resembling the typical behavior of metals in small magnetic fields. As revealed in previous studies,[9,32–34] the magnetoconductance of the depleted $LaAlO_3$-$SrTiO_3$ interface shows a negative derivative in low fields and a positive in high fields (green curve). This behavior has been interpreted as the result of spin-orbit interaction and weak localization.[34] Near the MIT, in contrast, the magnetoconductance is always positive and has a negative second derivative in high fields (blue curve).

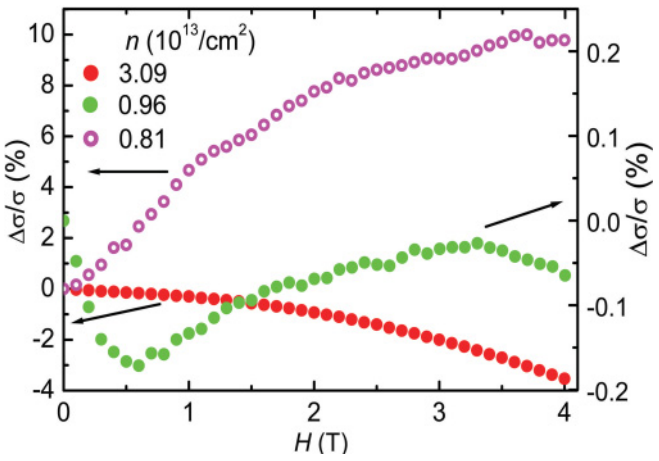

FIG. 5. (Color online) Magnetoconductance of the 25-μm sample shown in Fig. 4(a) measured at 4.2 K. Due to the large Hall voltage in the depleted state, the conductance is symmetrized using $[\sigma(H) + \sigma(-H)]/2$. From high to low carrier density, the corresponding reduced carrier densities, δn, are 2.96, 0.23, and 0.03, respectively.

IV. CONCLUSION

In summary, the transport properties of $LaAlO_3$-$SrTiO_3$ interfaces were measured as a function of the mobile carrier density altered by gate fields. It is found that below a critical carrier density $n_c \sim 1 \times 10^{13}/cm^2$ the interfaces become insulating for small in-plane electric field. For samples with 4-uc-thick $LaAlO_3$ layers, this transition occurs at a conductivity of order e^2/h. For a wide range of temperatures, the dependencies of the conductivity on the reduced carrier density follow a $\sigma_0 \propto (n - n_c)/n_c$ characteristic.

While it remains to be explored, which of the proposed microscopic mechanisms, such as disorder potentials or polaronic enhancement of Wigner localization, determine the nature of the MIT, it is evident that the MIT in $LaAlO_3$-$SrTiO_3$ interfaces differs qualitatively from the one in two-dimensional semiconductor systems.

ACKNOWLEDGMENTS

The authors gratefully acknowledge fruitful discussions with T. Nattermann and financial support by the DFG (TRR 80, SFB 608) and the EU (oxIDes).

APPENDIX

Before the measurement, all samples are kept in a dark cryostat over night to minimize the effect of photoconductivity. Cooling is done with a rate of a few Kelvin per minute to avoid trapped charges in the devices. The transport properties are measured by a source meter (Keithley, model 2400) and a multimeter (Keithley, model 2000). In case the carrier density is less than n_c, an electrometer (Keithley, model 6514) is used. We found that the application of positive back-gate voltage alters the electronic behavior of the as-grown $LaAlO_3$-$SrTiO_3$ interface. However, the $\sigma_0(n)$ characteristics with and without the influence of the positive back-gate voltage still merge well. The values of n_c of all seven samples are shown in Table I.

In Fig. 6, the zero-bias conductivities (σ_0) of all seven devices in $LaAlO_3$-$SrTiO_3$ interfaces are shown as function of the carrier density. Since the conductivity in the vicinity of the MIT is highly sensitive to the variation of the back-gate voltage, we cannot conclude on the possible existence of a minimum σ_0 of different devices at different temperatures. While all devices with 4-uc-thick $LaAlO_3$ layers have the same

TABLE I. The values of critical carrier density (n_c) and the values of σ_1 of all measured samples at several temperatures. The $\sigma_0(\delta n)$ dependence can be scaled by normalizing with σ_1. σ_1 is a fit parameter, optimized to merge the linear parts of the $\sigma_0(\delta n)$. Sample A and sample B correspond to the two samples with channel widths of 25 and 10 μm described in the main text, respectively. The in-plane configurations of sample B to sample G are the same.

	T (K)	σ_1 (10^{-5} S)	n_c (10^{13}/cm^2)
Sample A (4 uc)	3	3.8	0.72
Sample A (4 uc)	4	4.1	0.77
Sample A (4 uc)	14	3.5	0.76
Sample A (4 uc)	25	3.5	0.81
Sample A (4 uc)	35	3.2	0.86
Sample B (4 uc)	4	3.2	1.00
Sample B (4 uc)	10	3.0	0.98
Sample B (4 uc)	20	2.9	1.08
Sample B (4 uc)	30	2.6	1.08
Sample C (4 uc)	4	5.3	1.08
Sample C (4 uc)	10	5.0	1.07
Sample C (4 uc)	25	3.5	1.08
Sample C (4 uc)	50	3.2	1.42
Sample D (4 uc)	4	4.9	1.18
Sample D (4 uc)	37	3.7	1.41
Sample E (8 uc)	4	2.45	1.25
Sample F (8 uc)	4	0.95	0.98
Sample G (8 uc)	4	0.43	0.85
Sample G (8 uc)	15	0.39	1.02

$\sigma_0(n)$ characteristic, the data points of devices with 8-uc-thick $LaAlO_3$ layers are more disperse.

The $\sigma_0(n)$ data can be scaled by using the reduced carrier density $\delta n = (n - n_c)/n_c$, as shown in Fig. 7. For $0.05 < \delta n < 1$, in this range $\sigma_0 > e^2/h$, all data curves are characterized by a power-law behavior $\sigma_0 \propto \delta n^q$, with $q \sim 1$. However, temperature dependencies and sample dependencies still produce the scatter in Fig. 7. The sample dependence is more significant in the devices with 8-uc-thick $LaAlO_3$ layers.

The data can be further scaled by normalizing σ_0 with a parameter σ_1. By this normalization, the linear parts of the data curves in Fig. 7 are merged. The respective values of σ_1 are shown in Table I. For all devices with 4-uc $LaAlO_3$-$SrTiO_3$ interfaces, the carrier-density dependence of the conductivity follows a master curve, as shown in Fig. 8.

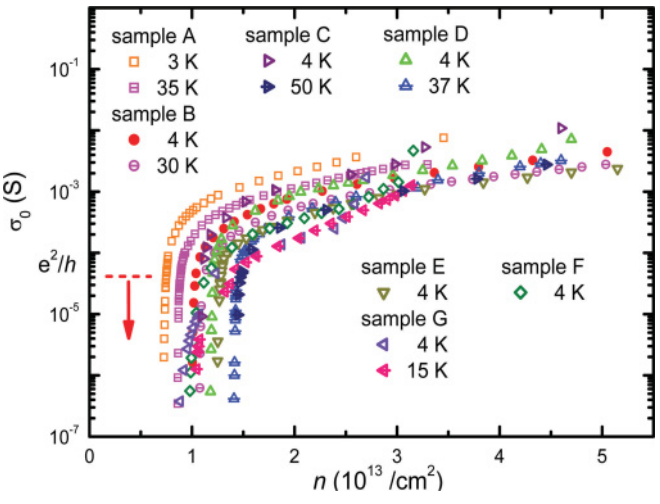

FIG. 6. (Color online) Conductivities of all seven devices in $LaAlO_3$-$SrTiO_3$ interface samples measured as function of the carrier density as controlled by V_G (in zero magnetic field). For clarity, not all data are shown. The critical carrier density n_c ranges from 0.5×10^{13}/cm^2 to 1.5×10^{13}/cm^2. Except for the data of the devices with 8-uc-thick $LaAlO_3$ layers (sample E to sample G), all data of devices with 4-uc-thick $LaAlO_3$ layers (sample A to sample D) have the same characteristic.

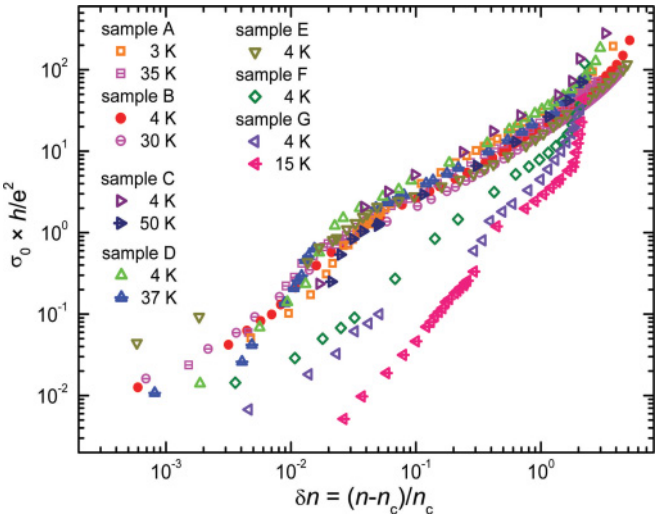

FIG. 7. (Color online) Conductivities of $LaAlO_3$-$SrTiO_3$ interface samples plotted as function of the reduced carrier density. The curve includes data points in the ohmic regime only. Sample A to sample D have 4-uc-thick $LaAlO_3$ layers, while sample E to sample G have 8-uc-thick $LaAlO_3$ layers.

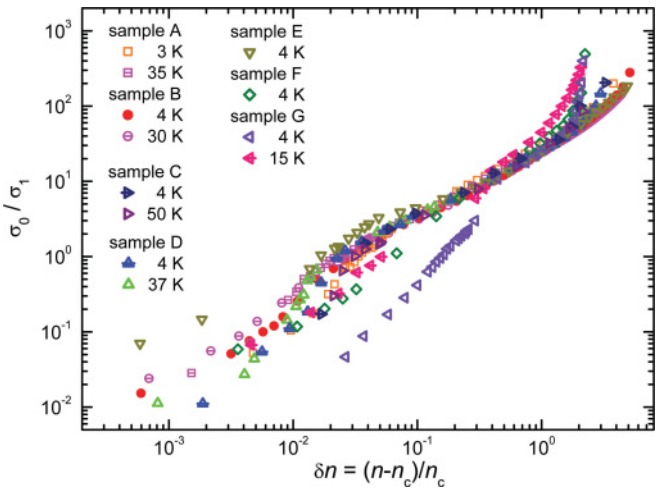

FIG. 8. (Color online) Normalized conductivities of $LaAlO_3$-$SrTiO_3$ interface samples plotted as function of the reduced carrier density. The conductivity is normalized by σ_1. The values of σ_1 are shown in Table I. Sample A to sample D have 4-uc-thick $LaAlO_3$ layers, while sample E to sample G have 8-uc-thick $LaAlO_3$ layers.

*jochen.mannhart@physik.uni-augsburg.de

[1] A. Ohtomo and H. Hwang, Nature (London) **427**, 423 (2004).
[2] A. D. Caviglia, S. Gariglio, C. Cancellieri, B. Sacépé, A. Fête, N. Reyren, M. Gabay, A. F. Morpurgo, and J.-M. Triscone, e-print arXiv:1007.4941 (2010).
[3] M. Huijben, G. Koster, H. J. A. Molegraaf, M. K. Kruize, S. Wenderich, J. E. Kleibeuker, A. McCollam, V. K. Guduru, A. Brinkman, H. Hilgenkamp, U. Zeitler, J. C. Maan, D. H. A. Blank, and G. Rijnders, e-print arXiv:1008.1896v1 (2010).
[4] M. Shalom, A. Ron, A. Palevski, and Y. Dagan, Phys. Rev. Lett. **105**, 206401 (2010).
[5] D. Rakhmilevitch, M. Shalom, M. Eshkol, A. Tsukernik, A. Palevski, and Y. Dagan, e-print arXiv:1009.1273 (2010).
[6] M. Breitschaft, V. Tinkl, N. Pavlenko, S. Paetel, C. Richter, J. R. Kirtley, Y. C. Liao, G. Hammerl, V. Eyert, T. Kopp and J. Mannhart, Phys. Rev. B **81**, 153414 (2010).
[7] N. Reyren, S. Thiel, A. D. Caviglia, L. Fitting Kourkoutis, G. Hammerl, C. Richter, C. W. Schneider, T. Kopp, A.-S. Rüetschi, D. Jaccard, M. Gabay, D. A. Muller, J.-M. Triscone and J. Mannhart, Science **317**, 1196 (2007).
[8] A. Brinkman, M. Huijben, M. van Zalk, J. Huijben, U. Zeitler, J. C. Maan, W. G. van der Wiel, G. Rijnders, D. H. A. Blank and H. Hilgenkamp, Nat. Mat. **6**, 493 (2007).
[9] A. D. Caviglia, S. Gariglio, N. Reyren, D. Jaccard, T. Schneider, M. Gabay, S. Thiel, G. Hammerl, J. Mannhart and J.-M. Triscone, Nature (London) **456**, 624 (2008).
[10] S. Thiel, G. Hammerl, A. Schmehl, C. W. Schneider, and J. Mannhart, Science **313**, 1942 (2006).
[11] C. Cen, S. Thiel, G. Hammerl, C. Schneider, K. Anderson, C. Hellberg, J. Mannhart, and J. Levy, Nat. Mater. **7**, 298 (2008).
[12] S. Thiel, C. W. Schneider, L. F. Kourkoutis, D. A. Muller, N. Reyren, A. D. Caviglia, S. Gariglio, J.-M. Triscone, and J. Mannhart, Phys. Rev. Lett. **102**, 046809 (2009).
[13] J. Mannhart and D. Schlom, Science **327**, 1607 (2010).
[14] E. Abrahams, P. W. Anderson, D. C. Licciardello, and T. V. Ramakrishnan, Phys. Rev. Lett. **42**, 673 (1979).
[15] L. Li, C. Richter, S. Paetel, T. Kopp, J. Mannhart, and R. C. Ashoori, e-print arXiv:1006.2847v2 (2010).
[16] At the $LaAlO_3$ $SrTiO_3$interface, the Fermi energy equals approximately 10 meV. This applies for $n \sim 10^{13}/\mathrm{cm}^2$ and $m^*/m_e \sim 3$. Below 50 K, the oxide interfaces therefore do not reach the Fermi temperature. The kinetic energy per particle $E_{\mathrm{kin}} \propto n$ and the Coulomb interaction $V \propto n^{1/2}$, so $V/E_{\mathrm{kin}} \sim 100/\varepsilon$. With a dielectric constant $\varepsilon \sim 5-10$ we conclude that the Coulomb energy exceeds the kinetic energy by an order of magnitude, similarly to the semiconductor systems.
[17] S. V. Kravchenko, W. E. Mason, G. E. Bowker, J. E. Furneaux, V. M. Pudalov, and M. D'Iorio, Phys. Rev. B **51**, 7038 (1995).
[18] S. V. Kravchenko and M. P. Sarachik, Rep. Prog. Phys. **67**, 1 (2004).
[19] V. Dobrosavljević, E. Abrahams, E. Miranda, and S. Chakravarty, Phys. Rev. Lett. **79**, 455 (1997).
[20] D. Popović, A. B. Fowler, and S. Washburn, Phys. Rev. Lett. **79**, 1543 (1997).
[21] Y. Meir, Phys. Rev. Lett. **83**, 3506 (1999).
[22] A. A. Pastor and V. Dobrosavljević, Phys. Rev. Lett. **83**, 4642 (1999).
[23] B. L. Altshuler and D. L. Maslov, Phys. Rev. Lett. **82**, 145 (1999).
[24] S. Washburn, N. Kim, X. Feng, and D. Popović, Ann. Phys. **8**, 569 (1999).
[25] L. A. Tracy, E. H. Hwang, K. Eng, G. A. Ten Eyck, E. P. Nordberg, K. Childs, M. S. Carroll, M. P. Lilly, and S. Das Sarma, Phys. Rev. B **79**, 235307 (2009).
[26] C. Bell, S. Harashima, Y. Kozuka, M. Kim, B. G. Kim, Y. Hikita, and H. Y. Hwang, Phys. Rev. Lett. **103**, 226802 (2009).
[27] M. Kawasaki, K. Takahashi, T. Maeda, R. Tsuchiya, M. Shinohara, O. Ishiyama, T. Yonezawa, M. Yoshimoto and H. Koinuma, Science **266**, 1540 (1994).
[28] G. Koster, B. L. Kropman, G. J. H. M. Rijnders, D. H. A. Blank, and H. Rogalla, Appl. Phys. Lett. **73**, 2920 (1998).
[29] C. W. Schneider, S. Thiel, G. Hammerl, C. Richter, and J. Mannhart, Appl. Phys. Lett. **89**, 122101 (2006).
[30] We use the word "ohmic" following the usage to describe $J(E)$ characteristics with a finite conductance at $E = 0$. $J(E)$ characteristics in which $J \propto E$ are called "linear."
[31] P. H. Kes and C. C. Tsuei, Phys. Rev. B **28**, 5126 (1983).
[32] C. Bell, S. Harashima, Y. Hikita, and H. Y. Hwang, Appl. Phys. Lett. **94**, 222111 (2009).
[33] M. Ben Shalom, M. Sachs, D. Rakhmilevitch, A. Palevski, and Y. Dagan, Phys. Rev. Lett. **104**, 126802 (2010).
[34] A. D. Caviglia, M. Gabay, S. Gariglio, N. Reyren, C. Cancellieri, and J.-M. Triscone, Phys. Rev. Lett. **104**, 126803 (2010).